Strojniški vestnik - Journal of Mechanical Engineering 68(2022)4, 240-251
DOI:10.5545/sv-jme.2022.26
Original Scientific Paper, Special Issue: SARS-CoV-2
Received for review: 2022-01-23
Received revised form: 2022-03-04
Accepted for publication: 2022-03-04

Comparison Study of Four Commercial SARS-CoV-2-Rapid Antigen Tests: Characterisation of the Individual Components

Žiga Jelen – Ivan Anžel – Rebeka Rudolf*
University of Maribor, Faculty of Mechanical Engineering, Slovenia

During the corona virus (COVID-19) pandemic, there was a sharp increase in the need for diagnostic tests that could detect the presence of SARS-CoV-2 virus or its antibodies quickly and reliably. An important type in the group of diagnostic tests are rapid antigen lateral flow immuno-assay (LFIA) tests, which operate on the immuno-chromatographic principle with the lateral flow of analyte. Clinical practice in the last year has shown that such diagnostic tests can be effective in preventing the spread of the SARS-CoV-2 virus.

The development, and, thus, the production of the rapid antigen LFIA tests, is influenced by a number of factors that determine their sensitivity and accuracy indirectly. These factors are directly dependent on the type of antibody produced, which is formed as an immune response when infected with the virus. The production of the rapid antigen LFIA tests is associated with the appropriate selection of basic components that determine the type and quality of these tests. The basic components include: substrates and membranes, antigens, antibody labels and compatible buffers. The correct choice of membranes and their materials is crucial to compiling an effective rapid antigen LFIA test.

This study therefore presents a comparative analysis of four commercially available SARS-CoV-2-rapid LFIA tests using state-of-the-art characterisation techniques scanning electron microscopy (SEM), inductively coupled plasma-optical emission spectrometry (ICP-OES), environmental scanning electron microscope / energy-dispersive X-ray spectroscopy (ESEM/EDX), Fourier-transform infrared spectroscopy / attenuated total reflection (FTIR/ATR) for the individual components. The obtained results were the starting point for the development and assembling of our own rapid antigen LFIA test based on gold nanoparticles as antibody labels.

Keywords: rapid antigen test, components, characterisation, analysis

Highlights

- *The characteristic of commercially available SARS-CoV-2-rapid LFIA tests were studied.*
- *The structures and morphology of the pads (sample, conjugate, additional pad, absorbtion) were described.*
- *The Au content in the conjugate pad varies between 0.05 µg to 0.12 µg.*
- *The presence of the impurities: Ca, Al, Si, K, Fe and Ni was detected by ESEM/EDS analysis on fibre surfaces in the conjugated pads.*
- *The total time until the control line becomes visible varies between 42.5 s to 86.77 s.*

0 INTRODUCTION

Given the severity, speed and complexity of the transmission of SARS-CoV-2 virus, it is particularly important for early diagnosis and understanding of the epidemiological characteristics of the disease, to ensure the safety of the population while reducing disease transmission. The field that offers innovative solutions to many clinical problems related to the diagnosis, treatment and prevention of COVID-19 is the field of Nanotechnology and the use of nanomaterials for virus detection. Among nanomaterials, gold nanoparticles (AuNPs) are the most promising, as they have unique optical properties associated with localised surface plasmon resonance, and, at the same time, they are highly biocompatible **[1]** and **[2]**. AuNPs can also be used use in medicine and biomedicine, especially in diagnosing viruses, bacteria, as well as in the treatment of cancer. In order to prevent the spread of COVID-19, a fast and reliable diagnosis is a must **[3]** to **[6]**.

Lateral flow immuno-assay (LFIA) is a quick and easy method to detect various analytes (viruses, antibodies, bacteria, hormones, etc.) in various samples, such as blood, urine, saliva, serum, plasma. The result of the test is shown in only a few minutes, and the result itself is the signal (colour) of the test area test line, which is most often marked as ''T''. The indicating pigment is formed from protein conjugates with AuNPs, that can bind selectively to specific proteins or molecules **[7]**. These are later immobilised on a thin line when they are captured by surface bound antigen molecules on the test line. AuNPs, namely, give quantitative and/or semi-quantitative responses, and, with that, a direct signal soon after the reaction with the proteins.

Rapid antigen LFIA tests present an important aspect in preventing the spread of the diseases such as SARS-CoV-2 coronavirus (COVID-19) **[8]**. The principle of operation of a typical LFIA test is simple: A liquid sample (or an extract thereof) containing the analyte is applied to a sample pad that acts like a sponge, as it retains the excess liquid sample. After

*Corr. Author's Address: University of Maribor, Faculty of Mechanical Engineering, Smetanova ulica 17, 2000 Maribor Slovenia, rebeka.rudolf@um.si

wetting the sample pad, the sample begins to move laterally due to capillary action - first to a conjugate pad containing the applied dry AuNPs or a similar marker (e.g., latex, silica, carbon) [9] conjugated to a specific protein such as the SARS-CoV-2 Spike S1 antigen, and AuNPs conjugated to monoclonal recombinant IgG antigens (e.g., rabbit, mouse, chicken) [10] and [11]. At this point, a chemical reaction (binding) occurs between the desired analyte and AuNPs conjugated to the SARS-CoV-2 Spike S1 antigen to form a complex. The antibody-conjugate/analyte complex is captured on the test line, which contains either an identical protein or similar antigens. The remaining AuNPs conjugated with the IgG antigen travel to the control line, which is most often marked: ''C'', and are immobilised, forming a line. After passing the sample across the membrane and test lines, the excess fluid or buffer is adsorbed into the absorbent pad.

If the target analyte is present, the test line will be coloured. The control line must be coloured even if the target analyte is not present, since this signifies the correct operation of the test.

Acute coronavirus 2 respiratory syndrome (SARS-CoV-2) leads to the infectious disease COVID-19, first reported in Wuhan, China in December 2019. Since then, the disease has spread worldwide. SARS-CoV-2 is a highly contagious virus and spreads to humans through the respiratory tract, especially through droplets, aerosols, and contact with contaminated surfaces [12]. The number of virus replicates was estimated to be about 2.68, with a doubling time of 6.4 days. Its incubation period from infection to the first symptoms in a person is, on average, 5 to 14 days [13] and [14].

SARS-CoV-2 is a single-stranded, positive-directional RNA virus. The virus belongs to the genus beta-coronaviruses, and has a diameter of 50 nm to 200 nm. SARS-CoV-2 is characterised by spike glycoproteins that protrude from its surface and give it its characteristic appearance. The SARS-CoV-2 genome encodes four major structural and functional proteins: Thorns (S), membrane (M), envelope (E), and nucleocapsid (N) proteins. Protein S consists of two functional subunits, S1 and S2; S1 is responsible for recognising and binding the host cell receptor, i. angiotensin 2 conversion enzyme (ACE2) [15], while S2 mediates membrane fusion. Protein M is the most common structural protein that determines the shape of the virus. Protein N is the most secreted viral protein among infections, and can be detected in serum and urine samples during the first two weeks of infection. The smallest major structural protein is E, which is involved in the virus assembly and pathogenesis [16] and [17]. Lateral traction analysis allows qualitative virus detection. Such tests have many advantages for rapid diagnostic testing of COVID-19, as they are simple, affordable, require minimal sample volumes (10 µL to 20 µL), do not require additional analytical equipment and give results in minutes [18].

A key requirement for LFIA rapid antigen tests set by the World Health Organization is that they have at least 90 % diagnostic sensitivity. In the case of diagnostic performance compared with the device used as a reference, the diagnostic sensitivity must be at least equivalent to the reference devices as defined in Directive 98/79/EC. The diagnostic specificity must be at least 98 %. Assessments of diagnostic specificity and diagnostic sensitivity must have at least 95 % confidence intervals [19]. In this study, we compared four commercially available rapid antigen LFIA tests using state-of-the-art characterisation techniques for individual components, with the aim of identification their chemical composition and other properties that are crucial for the operation of these tests.

1 EXPERIMENTAL

Four (4) LFIA rapid antigen tests from different manufacturers were evaluated according to their individual components, their chemical composition, morphology and structure. The following rapid tests were examined, as presented in Table 1. Particular attention was focused to the investigation of a conjugate pad containing dry antigens conjugated with AuNPs.

To achieve a concise overview of their manufacture we used the following analytical methods:

Table 1. *List of the Sars-Cov-2 LFIA antigen rapid tests*

Short name	Full name	Manufacturer
Acro	ACRO Rapid Test	ACRO BIOTECH, Inc.
Citest	Citest	CITEST DIAGNOSTICS INC.
Singclean	Singclean IVD COVID-19 Test Kit (Colloidal Gold Method)	Hangzhou Singclean Medical Products Co., Ltd.
UNscience	UNscience SARS-CoV-2 Antigen Rapid Test	Wuhan UNscience Biotechnology Co., Ltd.

1.1 Scanning Electron Microscopy (SEM)

SEM (SEM, FEI Sirion 400 NC, FEI Technologies Inc., Hillsboro, Oregon, USA) was used for observation of all the different membranes` structures (sample pad, conjugate pad, additional pad, chromatographic membrane, absorbtion pad) from the chosen rapid antigen LFIA tests. The samples were glued onto graphite holders. To minimise static charging with the electron beam during SEM observations and to ensure sample conductivity, the samples were subsequently sputtered on a JFC-1100E ion sputter machine (Jeol, Akishima, Japan) with Au for 40 s at a distance of 3 cm from the Au source.

1.2 Inductively Coupled Plasma-Optical Emission Spectrometry (ICP-OES)

The ICP-OES (Agilent 720/725 ICP-OES, Agilent Technologies, Santa Clara, USA) analysis was used for the measurement of the Au content on the conjugate pads. The following procedure was performed in order to measure the Au concentration: The conjugate pads were removed from the test strips and immersed in 0.5 mL of Phosphate buffered saline (pH = 7.4, Sigma-Aldrich Chemie GmbH Steinheim, Germany) and sonicated for 15 min, in order to ensure adequate Au release. Prior to analysis, the sample was acidified with aqua regia, and the analysis was performed at the following operating parameters: RF power: 1.5 kW, nebuliser: Meinhard, plasma flow: 15 L/min, nebuliser flow gas: 0.85 L/min, make up gas flow: 0.28 L/min, reaction gas flow: 4.0 mL/min. Calibration of the instrument was performed with matrix standard calibration solutions. The relative measurement uncertainty was estimated to be ± 3 %.

1.3 Environmental Scanning Electron Microscope (ESEM) with Energy Dispersion Spectrometer (EDS)

An ESEM (Thermo Fischer Scientific, environmental Prisma-E) was used in an attempt to evaluate the structure and composition of the conjugate pads. The purpose of this observation was to obtain information on the volume distribution and potential type of surface binding of AuNPs. Samples were non-coated, and analysed at 40 Pa to avoid degassing and vacuum drying of the sample. An EDX semi-qualitative analysis using a detector (EDS Oxford INCA 350) was performed to obtain information about the chemical composition and distribution of the individual elements (as element mapping). EDS mapping was performed in an attempt to differentiate Au from the background.

1.4 LFIA Test Duration

The speed of the chosen rapid antigen LFIA tests` duration was measured by using the tests as intended, and as described in the accompanying instructions with just their supplied buffer solution. The start time was taken when the first drop was placed into the sample well, and the end time just as the control line began to become visible. This was done on 6 consecutive tests for each different test to get an average value.

1.5 Fourier-Transform Infrared Spectroscopy (FTIR) with Attenuated Total Reflection (ATR)

The chemical composition of the membranes for all chosen rapid antigen LFIA tests was determined with FTIR (Spectrum 3, Perkin Elmer, Waltham, USA) and ATR (GladiATR, Pike Technologies, Fitchburg, USA) spectroscopy. The samples were placed face up on the ATR crystal, so as to avoid the adhesive backing that is used in rapid antigen LFIA tests. The samples were scanned in the range of 650cm^{-1} to 4000 cm^{-1}, with 4 samples` scans.

2 RESULTS

2.1 Scanning Electron Microscopy (SEM)

SEM micrographs of all membranes` structures from the sample pad, conjugate pad, additional pad and chromatographic membrane were taken at comparative and identical magnifications. In this way, an insight was obtained into the structure and morphology of each component.

SEM analysis revealed that the sample pads were composed of interwoven glass fibres, together with a binder (Figs. 1a to 4a). The diameter of the glass fibres bottles was a few μm.

SEM analysis of the conjugate pads showed that they were also composed of fibres, which had a bigger diameter of some 10 μm. The use of inert materials in the conjugate pad is crucial, as they must ensure low non-specific binding to the analytes, allow a constant and even flow of the sample, as well as a consistent volume of reagent / buffer [20] and [21]. The conjugate pads in the Acro and Citest rapid antigen tests were composed of organic polymer fibres (Figs. 1b and 2b), compared to the Singclean and UNscience rapid tests (Figs. 3b and 4b) which had a fibreglass-based pad.

The Acro and Citest tests had an additional pad (Figs. 1c and 2c), with similar structural and morphological properties as the conjugate pad. Examination showed that it was composed of tightly woven polymer fibres. Its intended function was most likely as a filter pad, meant to protect the fine-pores of the chromatographic membrane.

The surface of the chromatographic membranes of the Acro and Citest tests (Figs. 1d and 2d) were visibly more uniform in morphology when compared to the Singclean and UNscience tests (Figs. 3c and 4c). It is a representation of a homogeneous network structure. Due to such a surface topology, these rapid antigen tests have a larger surface area in the chromatographic membranes. In contrast, at larger magnifications, the finer pore sizes of the Acro and Citest tests (Figs. 1e and 2e) clearly indicate that they have a significantly higher available surface area. The surface area in the

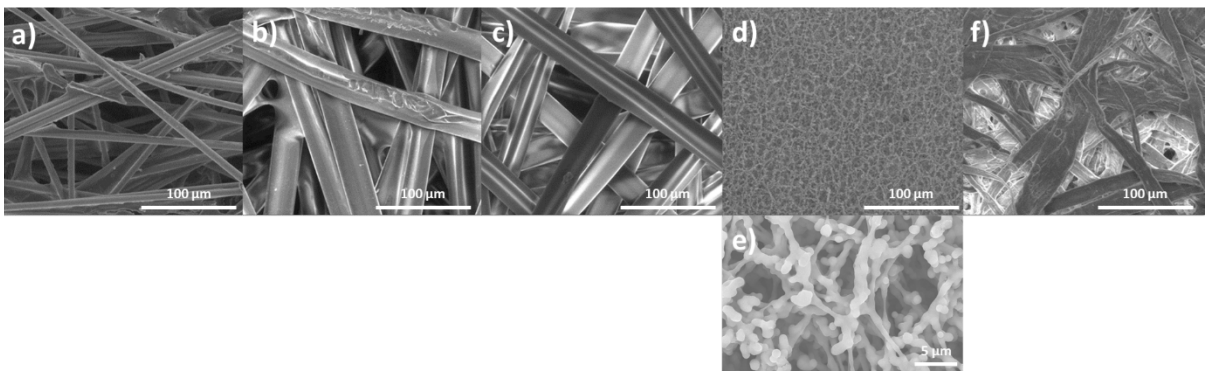

Fig. 1. *SEM micrographs of the Acro rapid antigen test membranes: a) sample pad, b) conjugate pad, c) additional pad, d) chromatographic membrane, e) detail from the chromatographic membrane, f) absorption pad*

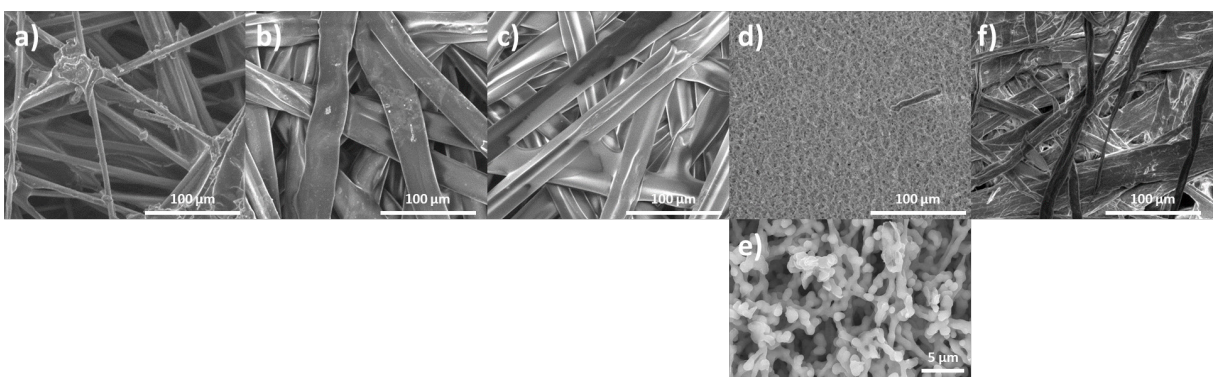

Fig. 2. *SEM micrographs of the Citest rapid antigen test membranes: a) sample pad, b) conjugate pad, c) additional pad, d) chromatographic membrane, e) detail from the chromatographic membrane, f) absorption pad*

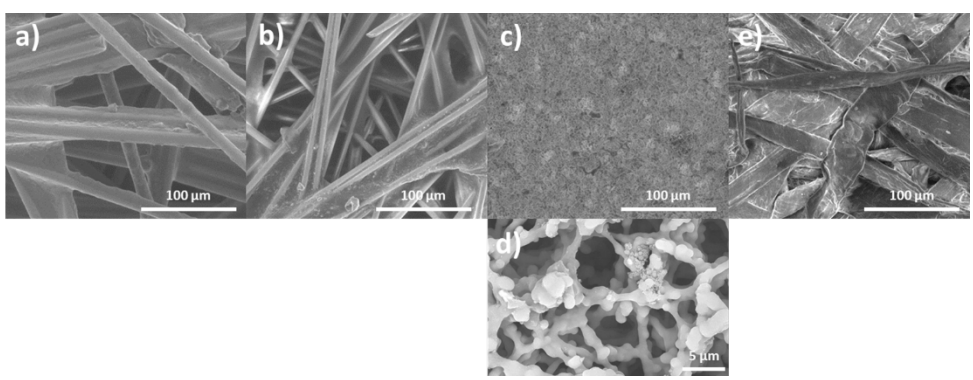

Fig. 3. *SEM micrographs of the Singclean rapid antigen test membranes: a) sample pad, b) conjugate pad, c) chromatographic membrane, d) detail from the chromatographic membrane, e) absorption pad*

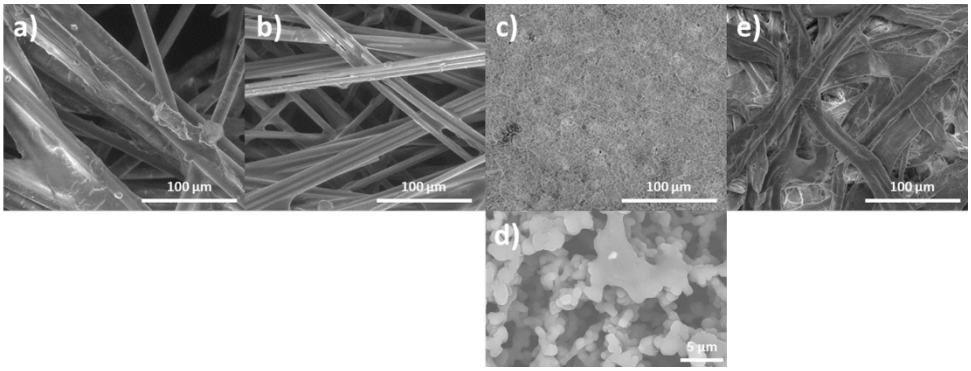

Fig. 4. *SEM micrographs of the Singclean rapid antigen test membranes: a) sample pad, b) conjugate pad, c) chromatographic membrane, d) detail from the chromatographic membrane, e) absorption pad*

chromatographic pad was of concern, since it dictates the degree to which it is possible to bind the binding biomolecules to the membrane. This is the place where the binding between the nitrocellulose esters and protein dipoles takes place [21] and [22] with an average diameter of approximately 18 nm. We used the conjugation between AuNPs and MAbs against SSd to prepare immunochromatographic strips (ICSs.

The SEM micrographs show that the structure of the absorption pads was almost similar, and no porosity was observed (Figs. 1f and 4f). The fibres were non-uniform in width and compressed in several planes.

2.2 Inductively Coupled Plasma-Optical Emission Spectrometry (ICP-OES)

Table 2 shows the average Au content in each rapid antigen test, obtained indirectly by the ICP-OES method. The results suggest that the Au content in the rapid antigen test varies between 0.05 µg to 0.12 µg on a single conjugate pad. The lower concentration of Au in the Acro and Citest tests also suggests higher colour intensity and plasmonic resonance in the AuNPs that were used [23] and [24].

Table 2. *Au content on single conjugate pads*

Test	m (Au) on single conjugate pad [μg]
Acro	0.055
Citest	0.05
Singclean	0.125
UNscience	0.105

2.3 Environmental Scanning Electron Microscope (ESEM) with energy dispersion spectrometer (EDS) mapping

ESEM by using EDS quantitative analysis was performed to determine the distribution of individual elements to gain insight into the elemental mapping on the fibre surface of the conjugate pad.

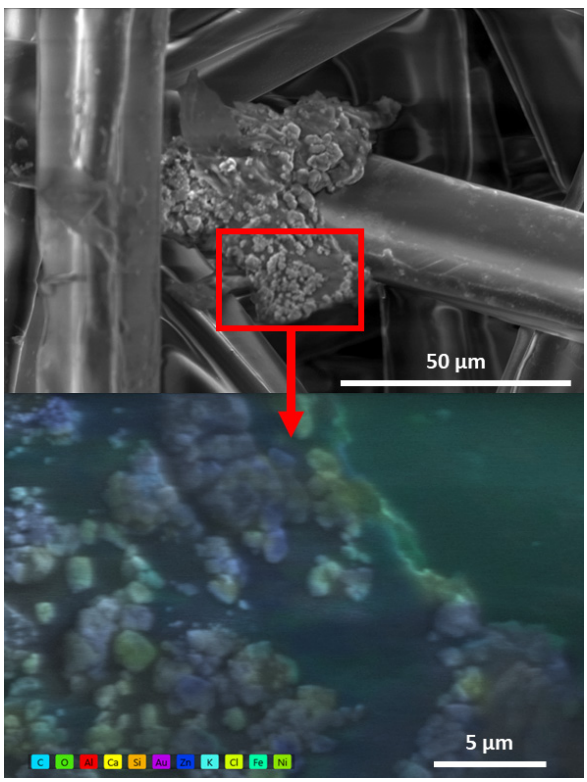

Fig. 5. *ESEM/EDS elemental mapping on the fibre from the conjugate pad (Acro rapid antigen test)*

Fig. 5 shows the EDS elemental mapping of the area on the fibre surface (as presented with the red frame) of the Acro rapid antigen test conjugate pad.

The analysis confirmed the presence of ZnCl on the fibre surface, as well as carbon and oxygen, which are present throughout the analysed area and originated from the polymer base. No Au was detected in this rapid antigen test, as well as no impurities such as e.g. Ca, Al, Si, K, Fe and Ni.

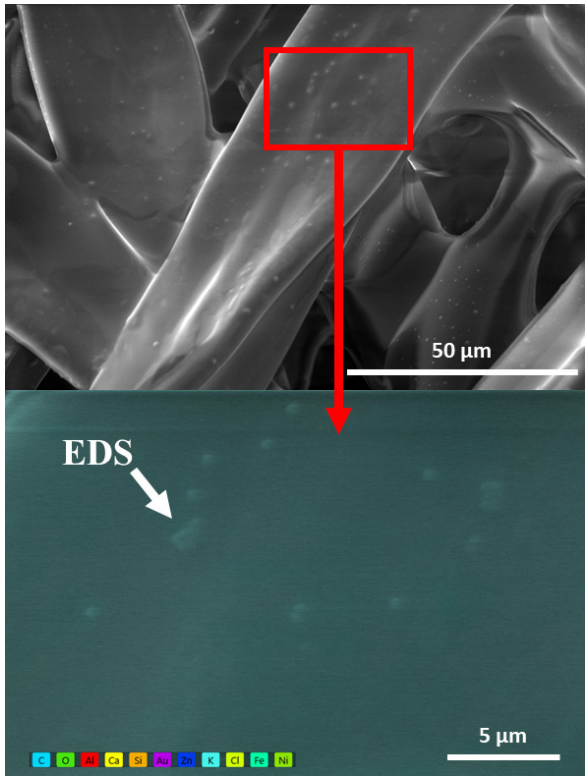

Fig. 6. *ESEM/EDS elemental mapping on the fibre from the conjugate pad (Citest rapid antigen test)*

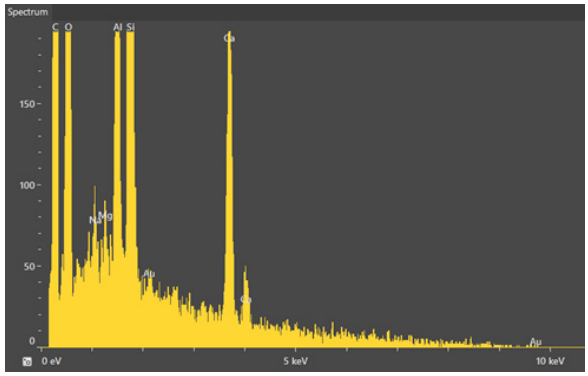

Fig. 7. *EDS spectrum of the surface spots - link Fig. 6*

Fig. 6 shows the EDS elemental mapping of the area on the fibre surface of the conjugate pad of the Citest rapid antigen test. Carbon and oxygen are present across the entire analysed area. Au and impurities such as Ca, Al, Si, K, Fe and Ni were

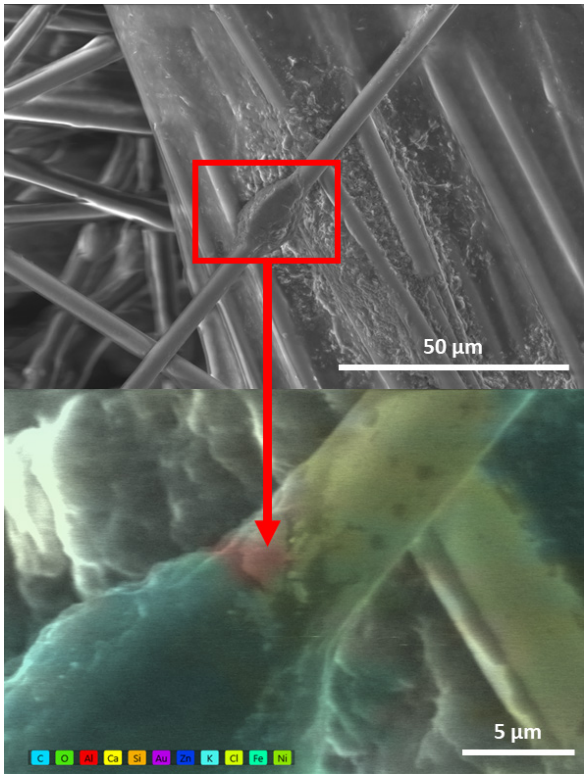

Fig. 8. *ESEM/EDS elemental mapping on the fibre from the conjugate pad (Singclean rapid antigen test)*

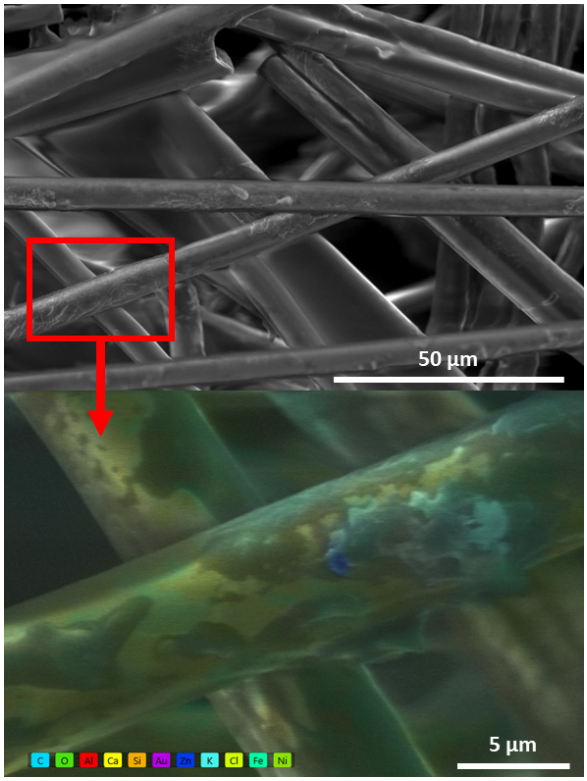

Fig. 9. *ESEM EDS map of the UNscience test conjugate pad*

detected in trace amounts. The additional EDS point analysis shows that the spots on the fibre surface are rich in Al (see the spectrum in Fig. 7).

Fig. 8 shows the EDS elemental distribution of the region on the fibre surface of the Singclean rapid antigen test conjugate pad. The fibres appear to be rich in Si, Ca and Al. Au and impurities such as Ca, Al, Si, K, Fe and Ni were detected in traces at the sites of analysis. The fibres are mostly organic, consisting of O and C.

Fig. 9 shows the EDS elemental distribution of the area on the fibre surface of the UNscience rapid antigen test conjugate pad. The fibres appear to be rich in Si, Ca, K and Al. Au and additional impurities Fe and Ni were detected in traces at the analysis sites. Also, here, the analysis shows that the fibres are mostly organic, consisting of O and C.

Based on the revealed morphology of AuNPs, it can be concluded that the AuNPs were synthesised with the same technology.

2.4 LFIA Test Duration

The total test time of all SARS-CoV-2 antigen rapid tests was read from the instructions, and was, in almost all cases, recommended at about 20 min. This time is defined as required in order to ensure that all the reagents have time to be rehydrated, released, and can react with the target proteins.

Experiments with all the SARS-CoV-2 antigen rapid tests have shown that the total time until the control line becomes visible, was considerably shorter compared to the instructions (see Table 3). On this basis, the fact was established that the affinity between the conjugated AuNP and glass fibres was significantly lower. This means that it took significantly less time to colour the control line and its full visibility. The next important finding is that the time when the control line is completely coloured is of the essence. Namely, a faster time usually does not mean that a quick antigen test is better. Previous studies **[21]**, **[22]**, **[25]** and **[26]** have found the exact opposite, finding that the longer the analyte flow time, the longer the test time, the better the sensitivity of the rapid antigen test.

2.5 Fourier-Transform Infrared Spectroscopy (FTIR) with Attenuated Total Reflection (ATR)

FTIR/ATR spectra of the individual pads were performed in order to identify their composition. Since conjugate pads are coated with AuNPs` conjugates, before analysis they were washed with demineralised water and sonicated individually for 1 min in demineralised water.

The spectra of the individual sample pads for all rapid antigen tests as shown in Fig. 10, indicate that they are composed of silicon boron glass fibres. The EDX spectrums (from Part 2.3) suggest a similar composition. FTIR also revealed the presence of a polyester based binder **[27]**.

The spectra in Fig. 11 showed that both the Acro and Citest rapid antigen tests use a similar material for a polyester fibre-based conjugate pad **[27]**. In comparison, the spectra of the Singclean and UNscience conjugate pads, shown in Fig. 12, revealed that they are composed mainly of glass fibres. The spectra suggest that small residues of the binder remained. Most of the binder was likely removed during the washing steps. Both the Acro and Citest tests had an additional pad, placed after the conjugate pad. The chemical composition as identified by FTIR is shown in Fig. 13, and it was identical to the polyester based conjugate pads. The SEM micrographs, however, revealed a significantly finer pore size, suggesting these pads are used for filtration.

The chemical composition of the chromatographic membrane was similar in all the sampled tests. The spectra displayed in Fig. 14, reveal the content of a nitrated cellulose **[28]**. Analysis of the absorption pads revealed that they are composed of cellulose, as shown in Fig. 15.

3 DISCUSSION

Detailed analysis of the SEM micrographs showed that the available rapid antigen LFIA tests are

Table 3. *Time needed for the control line to become visible*

Test	*t* [s]							t [s]						
	t_1	t_2	t_3	t_4	t_5	t_6	Average	t_1	t_2	t_3	t_4	t_5	t_6	Average
Acro	52	55	52	60	57	54	55.00	56	59	54	60	59	56	57.33
Citest	55	60	60	62	63	55	59.17	74	80	91	83	78	78	80.67
Singclean	35	37	35	39	43	38	37.83	44	42	42	44	56	43	45.17
UNscience	41	42	38	40	28	32	36.83	44	45	46	49	33	38	42.50

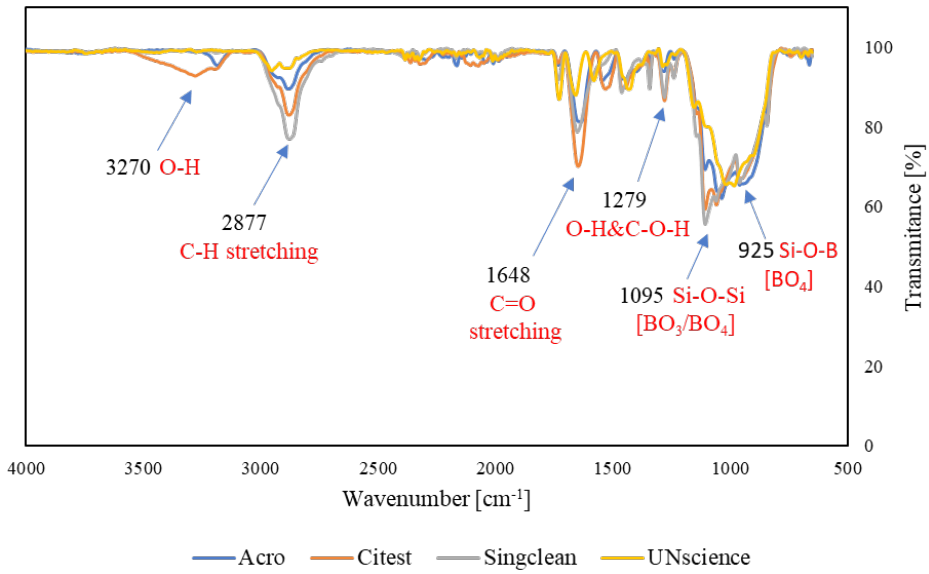

Fig. 10. *ATR-FTIR spectra of sample pads for all rapid antigen tests indicate the presence of glass fibres with a polyester-based binder*

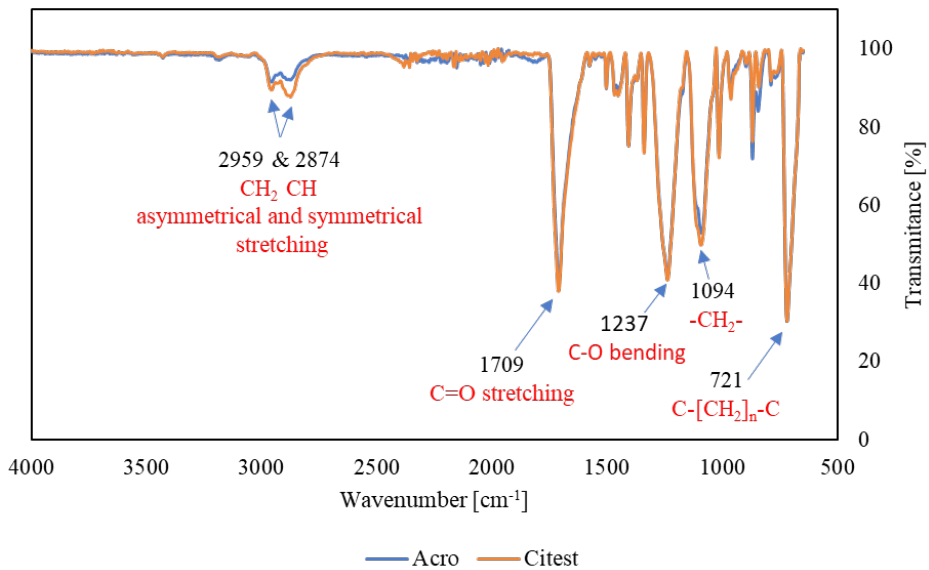

Fig. 11. *ATR-FTIR spectra of the conjugate pads from the Acro and Citest rapid antigen tests show the presence of polyester fibres*

generally similar in construction, not in the materials used, and with some special technical details such as the use of additional filter membranes. Comparative SEM/ESEM/EDX and FTIR/ATR analyses revealed that the use of fibrous materials was limited to polymers, cellulose, glass fibres and nitrocellulose. Investigations have shown, that nitrocellulose is an exclusive material that is used typically in chromatographic membranes.

The ESEM/EDS elemental mappings showed significant contaminations with impurities such as Ca, Al, Si, K, Fe and Ni in the conjugate pad. Whether this was a result of impurities in the reagents or residue from machinery cannot be determined at this point. The results of the impurity research show that LFIA rapid antigen tests are insensitive to impurities, although their concentration on the conjugate pad is not negligible. The presence of Si and Al, as detected by EDX analysis, and the presence of B-Si glass detected by FTIR, indicate that the glass fibres are based on the borosilicate glass of alumina.

A study of the individual components of four commercially available rapid antigen LFIA tests showed that the materials used for the key components

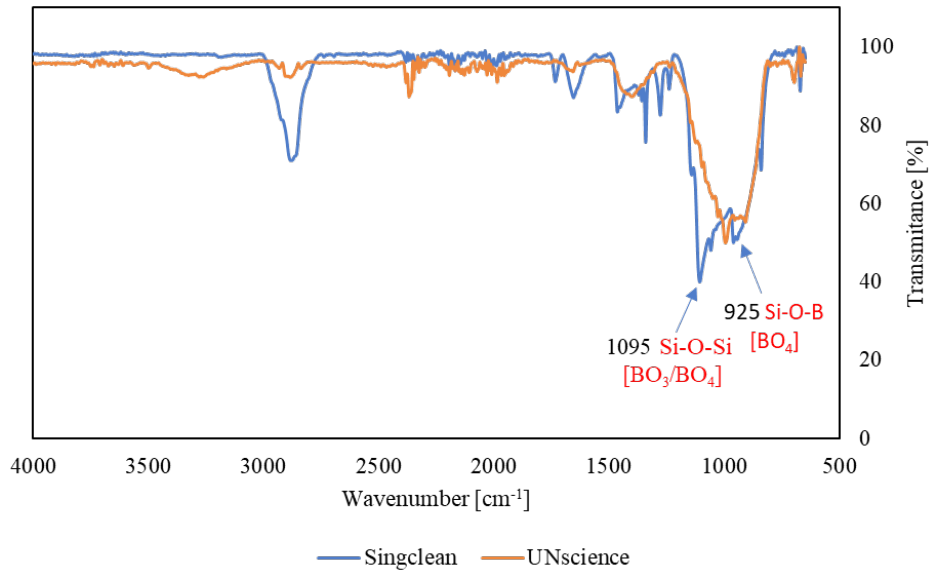

Fig. 12. *ATR-FTIR spectra of the conjugate pads from the Singclean and UNscience rapid antigen tests show the presence of glass fibres with a binder residue*

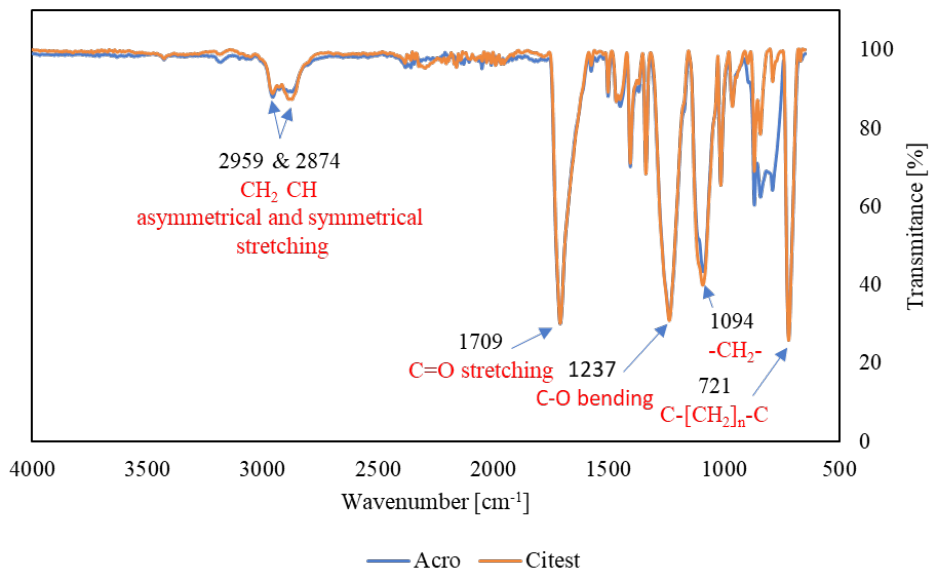

Fig. 13. *ATR-FTIR spectra of additional pads on the Acro and Citest rapid antigen tests*

are different. On the contrary, a review of the literature **[25]**, **[29]** and **[30]** showed that the materials currently used for development of rapid antigen LFIA tests are completely different.

The results of the SEM investigations showed that the selection of sample and conjugate pad material did not affect the performance of the rapid antigen LFIA test used significantly. The structure of the chromatographic membrane has the greatest influence on the sensitivity of the test, where the key factor is the size of the pores, which direct the performance, sensitivity and speed of the rapid antigen LFIA tests **[31]**.

The structure of the chromatographic membranes is homogeneous, with porous spaces about 5 µm in size, as can be seen from the SEM micrographs. From the results of an additional experiment that revealed the time required to obtain the coloured control line, it can be estimated that faster LFIA antigen tests have chromatographic membranes **[21]** with larger pores that are estimated to be > 5 µm.

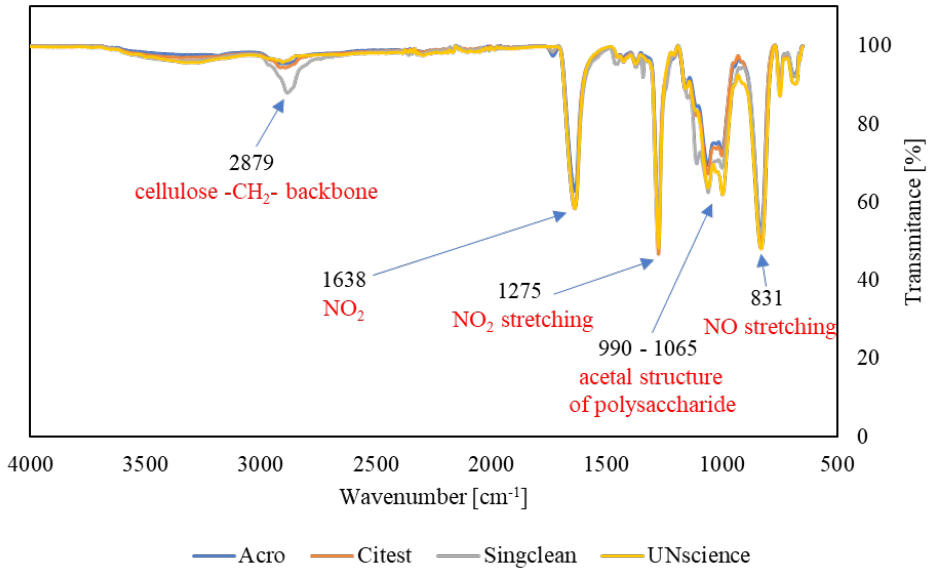

Fig. 14. *ATR-FTIR spectra of the nitrocellulose-based chromatographic pads for all the rapid antigen tests*

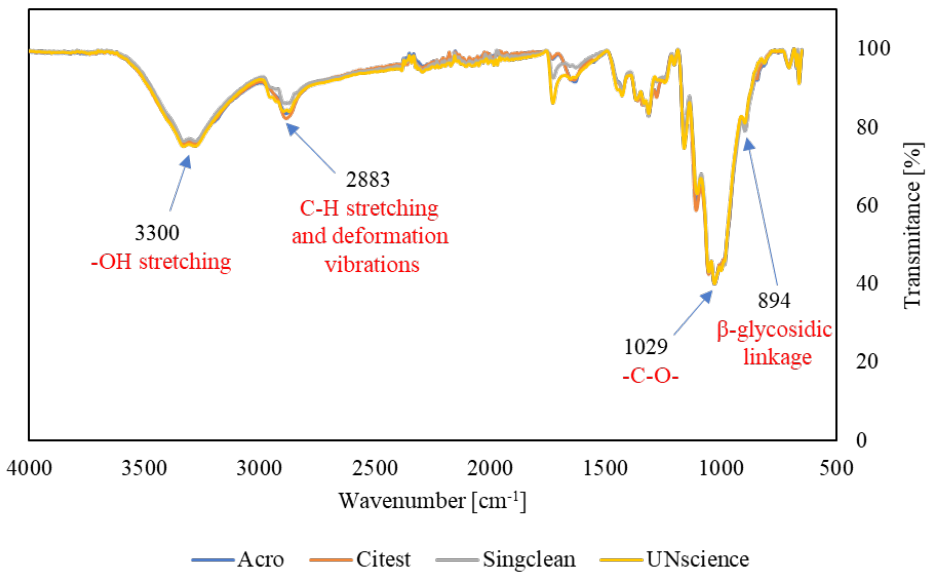

Fig. 15. *ATR-FTIR spectra of the cellulose-based absorption pads for all the rapid antigen tests*

Table 4. *Presentation of the materials identified in each component of the rapid antigen test*

Test	Sample pad	Conjugate pad	Filter pad	Chromatographic pad	Absorbtion pad
Acro	Glass fibre	Polyester	Polyester	Nitrocellulose	Cellulose
Citest	Glass fibre	Polyester	Polyester	Nitrocellulose	Cellulose
Singclean	Glass fibre	Glass fibre	//	Nitrocellulose	Cellulose
UNscience	Glass fibre	Glass fibre	//	Nitrocellulose	Cellulose

The performed analyses enabled the acquisition of the characteristics and properties of individual components of the rapid antigen LFIA tests, as well as their comparison. Based on this, the final Table 4 was prepared, which gives a quick insight into the analysed commercially available rapid antigen LFIA tests: Acro, Citest, Singclean and UNscience.

This study served as a basis for starting the development of an own rapid antigen LFIA test based on AuNPs for the detection of antibodies for the SARS-CoV-2 virus [32].

4 CONCLUSIONS

From this study the following conclusions can be drawn:

- Rapid antigen LFIA tests are complex in composition, as individual components have different chemical compositions and morphological characteristics, which ultimately results in different properties.
- For the pads in rapid antigen LFIA tests different materials are used, from glass fibre, polyster and cellulose.
- The choice of chromatographic membranes with larger pores does not affect the sensitivity of rapid antigen LFIA tests significantly.
- In order to know as accurately as possible the operation of rapid antigen LFIA tests, it is necessary to combine different characterisation techniques and experiments that can set up models, and, thus, a prediction for the most reliable operation in the clinical environment.

5 ACKNOWLEDGEMENTS

This research was funded by the Slovenian Research Agency, Grant number ARRS-Rpprog-JP-COVID-19-077 and Training and funding of a young researcher, (Co)financing Agreements no. 1000-19-0552, no. 1000-20-0552 and, no. 1000-21-0552. We thank Dr Peter Majerič for her help in conducting the research (SEM).

6 REFERENCES

[1] Sengani, M., Grumezescu, A.M., Rajeswari, V.D. (2017). Recent trends and methodologies in gold nanoparticle synthesis - A prospective review on drug delivery aspect. *OpenNano*, vol. 2, p. 37-46, **DOI:10.1016/j.onano.2017.07.001**.

[2] Rudolf, R., Majerič, P., Tomić, S., Shariq, M., Ferčec, U., Budič, B., Friedrich, B., Vučević, D. Čolić, M. (2017). Morphology, aggregation properties, cytocompatibility, and anti-inflammatory potential of citrate-stabilized AuNPs prepared by modular ultrasonic spray pyrolysis. *Journal of Nanomaterials*, vol. 2017, art. ID 9365012, **DOI:10.1155/2017/9365012**.

[3] Moitra, P., Alafeef, M., Dighe, K., Frieman, M.B., Pan, D. (2020). Selective Naked-eye detection of SARS-CoV-2 mediated by N gene targeted antisense oligonucleotide capped plasmonic nanoparticles. *ACS Nano*, vol. 14, no. 6, p. 7617-7627, **DOI:10.1021/acsnano.0c03822**.

[4] Wen, T., Huang, C., Shi, F.J., Zeng, X.Y., Lu, T., Ding, S.N., Jiao, Y.J.(2020). Development of a lateral flow immunoassay strip for rapid detection of IgG antibody against SARS-CoV-2 virus. *Analyst*, vol. 145, no. 15, p. 5345-5352, **DOI:10.1039/d0an00629g**.

[5] Li, Z., Yi, Y., Luo, X., Xiong, N., Liu, Y., Li, S., Sun, R., Wang, Y., Hu, B., Chen, W., Zhang, Y., Wang, J., Huang, B., Lin, Y., Yang, J., Cai, W., Wang, X., Cheng, J., Chen, Z., Sun, K., Pan, W., Zhan, Z., Chen, L., Ye, F. (2020). Development and clinical application of a rapid IgM-IgG combined antibody test for SARS-CoV-2 infection diagnosis. *Journal of Medical Virology*, vol. 92, no. 9, p. 1518-1524, **DOI:10.1002/jmv.25727**.

[6] Rabiee, Bagherzadeh, M., Ghasemi, A., Zare, H., Ahmadi, S., Fatahi, Y., Dinarvand, R., Rabiee, M., Ramakrishna, S., Shokouhimehr, M., Varma, R.S. (2020). Point-of-use rapid detection of SARS-CoV-2: Nanotechnology-enabled solutions for the covid-19 pandemic. *International Journal of Molecular Sciences*, vol. 21, no. 14. p. 1-23, **DOI:10.3390/ijms21145126**.

[7] Kim, D.S., Kim, Y.T., Hong, S.B., Kim, J., Heo, N.S., Lee, M.-K., Lee, S.J., Kim, B.I., Kim, I.S., Huh, Y.S., Choi, B.G. (2016). Development of lateral flow assay based on size-controlled gold nanoparticles for detection of hepatitis B surface antigen. *Sensors*, vol. 16, no. 12, art. ID 2154, **DOI:10.3390/s16122154**.

[8] Koczula, K.M., Gallotta, A. (2016). Lateral flow assays. *Essays in Biochemistry*, vol. 60, no. 1, p. 111-120, **DOI:10.1042/EBC20150012**.

[9] The NativeAntigen Company (2020). Choosing the Right Reagents for your Coronavirus Immunoassay Contents. The NativeAntigen Company, Kidlington, Oxford, from: *https://www.lubio.ch/assets/PDFs/Native_Antigen_Company_Choosing_The_Right_Reagents_for_Your_Coronavirus_Immunoassay.pdf*, accessed on 2021-01-15.

[10] Bahadır, E.B., Sezgintürk, M.K. (2016). Lateral flow assays: Principles, designs and labels. *Trends in Analytical Chemistry*, vol. 82, p. 286-306, **DOI:10.1016/j.trac.2016.06.006**.

[11] Grant, B.D. Anderson, C.F., Williford, J.R., Alonzo, L.F., Glukhova, V.A., Boyle, D.S., Weigl, B.H., Nichols, K.P. (2020). SARS-CoV-2 coronavirus nucleocapsid antigen-detecting half-strip lateral flow assay toward the development of point of care tests using commercially available reagents. *Analytical Chemistry*, vol. 92, no. 16, p. 11305-11309, **DOI:10.1021/acs.analchem.0c01975**.

[12] Yeasmin, M., Tasnim, J., Akram, A., Yusuf, M.A., Shamsuzzaman, A., Molla, M.M.A., Ghosh, A.K. (2020). Routes of Transmission of Newly Emerging SARS-CoV-2: A Systematic Review. *Bangladesh Journal of Infectious Diseases*, vol. 7, p. S18-S31, **DOI:10.3329/bjid.v7i0.46797**.

[13] Wu, J.T., Leung, K., Leung, G.M. (2020). Nowcasting and forecasting the potential domestic and international spread of the 2019-nCoV outbreak originating in Wuhan, China: a modelling study. *Lancet*, vol. 395, no. 10225, p. 689-697, **DOI:10.1016/S0140-6736(20)30260-9**.

[14] Sellner, J., Jenkins, T.M., von Oertzen, T.J., Sellner, J., Jenkins, T.M., von Oertzen, T.J., Bassetti, C.L., Beghi, E., Bereczki, D., Bodini, B., Cavallieri, F., Di Liberto, G., Helbok, R., Macerollo, A., Maia, L.F., Oreja-Guevara, C., Özturk, S., Rakusa, M., Pisani, A., Priori, A., Sauerbier, A., Soffietti, R., Taba, P., Zedde, M.,

Crean, M., Burlica, A., Twardzik, A., Moro, E. (2021). A plea for equitable global access to COVID-19 diagnostics, vaccination and therapy: The NeuroCOVID-19 Task Force of the European Academy of Neurology. *European Journal of Neurology*, vol. 28, **DOI:10.1111/ene.14741**.

[15] Huang, Y., Yang, C., Xu, X.F., Xu,W., wen Liu, S, (2020). Structural and functional properties of SARS-CoV-2 spike protein: potential antivirus drug development for COVID-19. *Acta Pharmacologica Sinica*, vol. 41, p. 1141-1149, **DOI:10.1038/s41401-020-0485-4**.

[16] Zou L., Ruan F., Huang M., Liang L. Huang H., Hong Z., Yu J.x, Kang M., Song Y., Xia J., Guo Q., Song T., He J., Yenz. H., Peiris M., Wu J. (2020). SARS-CoV-2 Viral load in upper respiratory specimens of infected patients (Correspondence). *The New England Journal of Medicine*, vol. 387, p. 1177-1179, **DOI:10.1056/NEJMc2001737**.

[17] Wang, Q., Zhang, Y., Wu, L. Niu, S., Song, C., Zhang, G., Qiao, C., Hu, Y., Yuen, K.Y., Wang, Q., Zhou, H., Yan, J., Qi, J. (2020). Structural and functional basis of SARS-CoV-2 entry by using human ACE2. *Cell*, vol. 181, no. 4, p. 894-904.e9, **DOI:10.1016/j.cell.2020.03.045**.

[18] Vashist S.K. (2020). In vitro diagnostic assays for COVID-19: Recent advances and emerging trends. *Diagnostics*, vol. 10, no. 4, art. ID. 202, **DOI:10.3390/diagnostics10040202**.

[19] Medical Devices. (2020). *MDCG 2021-2 Guidance on State of the Art of COVID-19 Rapid Antibody Tests*. p. 1-5, Medical Devices Coordination Group.

[20] Rozand, C. (2014). Paper-based analytical devices for point-of-care infectious disease testing. *European Journal of Clinical Microbiology & Infectious Diseases*, vol. 33, p. 147-156, **DOI:10.1007/s10096-013-1945-2**.

[21] Millipore, M. (2013). *Rapid Lateral Flow Test Strips Considerations for Product Development*. Merck Millipore. EMD Millipore Corporation, Billerica.

[22] Parolo, C., Senna-Torralba, A., Bergua, J.F., Bergua, J.F., Calucho, E., Fuentes-Chust, C., Hu, L., Rivas, L., Álvarez-Diduk, R., Nguyen, E.P., Cinti, S., Quesada-González, D., Merkoçi, A. (2020). Tutorial: design and fabrication of nanoparticle-based lateral-flow immunoassays. *Nature Protocols*, vol. 15, p. 3788-3816, **DOI:10.1038/s41596-020-0357-x**.

[23] Amendola, V., Pilot, R., Frasconi, M., Maragò, O.M., M. A. Iatì, M.A. (2017). Surface plasmon resonance in gold nanoparticles: A review. *Journal of Physics: Condensed Matter*, vol. 29, **DOI:10.1088/1361-648X/aa60f3**.

[24] Adekoya, J.A., Ogunniran, K.O., Siyanbola, T.O., Dare, E.O., Revaprasadu, N. (2018). Band structure, morphology, functionality, and size- dependent properties of metal nanoparticles. Noble and Precious Metals - Properties, Nanoscale Effects and Applications, Seehra, M.S., Bristow, A.D. (eds.). *IntechOpen*, p. 15-42, **DOI:10.5772/intechopen.72761**.

[25] Tomás, A.L., de ALmeida, M.P., Cardoso, F., Pinto, M., Rereira, E., Franco, R., Matos, O. (2019). Development of a gold nanoparticle-based lateral-flow immunoassay for Pneumocystis Pneumonia serological diagnosis at point-of-care. *Frontiers in Microbiology*, vol. 10, p. 1-20, **DOI:10.3389/fmicb.2019.02917**.

[26] Borse, V., Srivastava, R. (2019). Process parameter optimization for lateral flow immunosensing. *Materials Science for Energy Technology*, vol. 2, no. 3, p. 434-441, **DOI:10.1016/j.mset.2019.04.003**.

[27] Dos Santos Pereira, A.P., Da Silva, M.H.P., Lima, É.P., Dos Santos Paula, A., Tommasini, F.J. (2017). Processing and characterization of PET composites reinforced with geopolymer concrete waste. *Materials Research*, vol. 20, p. 411-420, **DOI:10.1590/1980-5373-MR-2017-0734**.

[28] Berthumeyrie, S., Collin, S., Bussiere, P.O., Therias, S. (2014). Photooxidation of cellulose nitrate: New insights into degradation mechanisms. *Journal of Hazardous Materials*, vol. 272, p. 137-147, **DOI:10.1016/j.jhazmat.2014.02.039**.

[29] Elahi, N., Kamali, M., Baghersad, M.H. (2018). Recent biomedical applications of gold nanoparticles: A review. *Talanta*, vol. 184, p. 537-556, **DOI:10.1016/j.talanta.2018.02.088**.

[30] Byzova, N.A., Zherdev, A.V., Khlebtsov, B.N., Burov, A.M., Khlebtsov, N.G., Dzantiev, B.B. (2020). Advantages of highly spherical gold nanoparticles as labels for lateral flow immunoassay. *Sensors*, vol. 20, no. 12, art. ID 3608, **DOI:10.3390/s20123608**.

[31] Mohit, E., Rostami, Z., Vahidi, H. (2021). A comparative review of immunoassays for COVID-19 detection. *Expert Review of Clinical Immunology*, vol. 17, no. 6, 2021, **DOI:10.1080/1744666x.2021.1908886**.

[32] Jelen, Ž., Majerič, P., Zadravec, M., Anžel, I., Rakuša, M., Rudolf, R. (2021). Study of gold nanoparticles' preparation through ultrasonic spray pyrolysis and lyophilisation for possible use as markers in LFIA tests. *Nanotechnology Reviews*, vol. 10, no. 1, p. 1978-1992, **DOI:10.1515/ntrev-2021-0120**.